ENDORF2 theory

The program is based on theory presented in [1, 2] for the simulation of single crystal and 'powder' ENDOR spectra. It was written with the purpose of analyzing spectra of free radicals for a general case when the nuclear quadrupole (*nqc*) and hyperfine (*hfc*) couplings of a nucleus may be of comparable magnitude.

A general theory to calculate ENDOR spectra of S=½ systems was employed under the assumption that the electron Zeeman interaction is dominating. No restrictions were made on the relative magnitudes of the *hfc* nuclear Zeeman and *nqc* splittings, the latter for nuclei with I>½. The energies and wave functions for each nucleus (i) with $I_i > ½$ were obtained by diagonalizing the perturbation Hamiltonian

$$H_i^{'} = \mathbf{I}_l \mathbf{A}_i \mathbf{u} S_u + \mathbf{I}_i \mathbf{Q}_i \mathbf{I}_i - \mu_N g_i \mathbf{B} \mathbf{I}_i,$$

where unit vector **u** is along the effective magnetic field direction. The principal axes of the *hfc* ($\mathbf{A}_i$) and *nqc* ($\mathbf{Q}_i$) tensors need not be parallel or coincide with the axes of the g-tensor. Spectra of radicals containing several nuclei (up to 10 in the present implementation) can be analyzed. The ENDOR transition frequencies were obtained as the energy difference between pairs of nuclear eigen-states belonging to the same m_S-value, + or - ½. In general the eigen-functions were mixtures of nuclear spin states. A simple formula, applicable for this case, was presented for the 1st order transition moment, including the effect of the *nqc* in single crystal and disordered systems. The method was applied for the analysis of experimental ENDOR spectra of radicals with anisotropic *hfc* and *nqc* splittings in disordered solids [1-5]. By taking into account angular selection as well as hyperfine enhancement the simulated spectra of radicals containing ^{1}H and/or ^{14}N nuclei became very similar to those obtained by matrix diagonalization [6] even when the *hfc* and *nqc* splittings were of comparable magnitude. This may be attributed to the use of formula (12) in [1] for the intensity in a powder sample. The method is therefore proposed as an alternative to the exact treatments [7, 8] for S = ½ systems provided that the high field approximation applies.

ENDORF2 code

The code is written in Fortran77 except for a few lines to read the computer clock (subroutine *gettim* available in Microsoft Fortran Powerstation). Diagonalisation of the Hamiltonian H_i' can be performed numerically for any nuclear spin in the range ½ ≤ I ≤ 9/2. An analytic treatment available for nuclei with I=1/2, 1, and 3/2 [9] is ca 30 % faster. The user interface to produce an input file is still under development as well as possibilities to specify multiple sites in single crystals. Any comments or suggestions on this version may be sent to:

Roland Erickson, Systems Development, SAAB Aeronautics, SAAB AB SE-581 88 Linköping, Sweden, E-mail: roland.erickson@comhem.se
Anders Lund Department of Physics, Chemistry and Biology, Linköping University, Husett, S-581 83 Linköping, Sweden, Email: anders.lund@liu.se

UPDATES

A few 'cosmetic' changes were made in the ENDORF2 code as follows:

- Hamiltonian is solved analytically by default for I < 2, numerically for I>3/2
- Direction cosine matrix is checked for orthogonality. Screen output warns for non-orthogonal vectors being automatically orthogonalized
- File names up to 30 characters are permitted
- Layout of interactively generated input file was improved

The changes were implemented in the **ENDORF2_7** code.

Provided files

- ENDORF2 program (source and executable files) for XP/Windows 7 on 32/64 bit PC
- ENDORF2_7 program (source and executable files)
- Text file with input description and examples of input data used for simulations shown below
- Copy of [1]
- Software for the plotting of spectra must be obtained separately and is not provided

References

1. Erickson R (1995) Electron Magnetic Resonance of Free Radicals. Theoretical and Experimental EPR, ENDOR and ESEEM Studies of Radicals in Single Crystal and Disordered Solids, Linköping Studies in Science and Technology, PhD Thesis No 391, ISBN 91-7871-582-2, Linköping, Sweden
2. Erickson R (1996) Simulation of ENDOR spectra of radicals with anisotropic hyperfine and nuclear quadrupolar couplings in disordered solids. Chem Phys 202:263-275
3. Erickson R, Lund A, Lindgren M (1995) Analysis of powder EPR and ENDOR spectra of the biphenyl radical cation on H-ZSM-5 zeolite, silica gel and in CFCl3 matrix Chem Phys 193:89-99
4. Erickson R, Benetis NP, Lund A, Lindgren M, (1997) Radical cation of naphthalene on H-ZSM-5 zeolite and in CFCl3 matrix. A theoretical and experimental EPR, ENDOR, and ESEEM study. J Phys Chem A 101:2390 –2396
5. Lund A, Erickson R (1998) EPR and ENDOR simulations for disordered systems: The balance between efficiency and accuracy. Acta Chem Scand 52:261–274
6. Erickson R, Lund A (2014) Applications of EPR and ENDOR Spectrum Simulations in Radiation Research. In Lund A, Shiotani M (eds) Applications of EPR in Radiation Research. Springer
7. (a) Stoll S, Schweiger A (2006) EasySpin, a comprehensive software package for spectral simulation and analysis in EPR. J Magn Reson 178:42–55; (b) EasySpin, version: 4.5.5 (2013) http://www.easyspin.org/ Accessed 2013-12-30
8. (a) Hanson GR, Noble CJ, Benson S (2013) XSophe - Sophe - XeprView and Molecular Sophe: computer simulation software suites for the analysis of continuous wave and pulsed EPR and ENDOR spectra. In: Lund A, Shiotani M (eds). EPR of free radicals in solids I, trends in methods and applications. Springer; (b) http://www.bruker.com/products/mr/epr/epr-software/epr-software.html Accessed 2014-01-13
9. Erickson R, Lund A (1991) Analytical Expressions of Magnetic Energies and Wavefunctions of Paramagnetic Systems with S=1/2 and I=1 or I=3/2. J Magn Reson 92:146-151

Examples of simulated powder ENDOR spectra with ENDORF2:

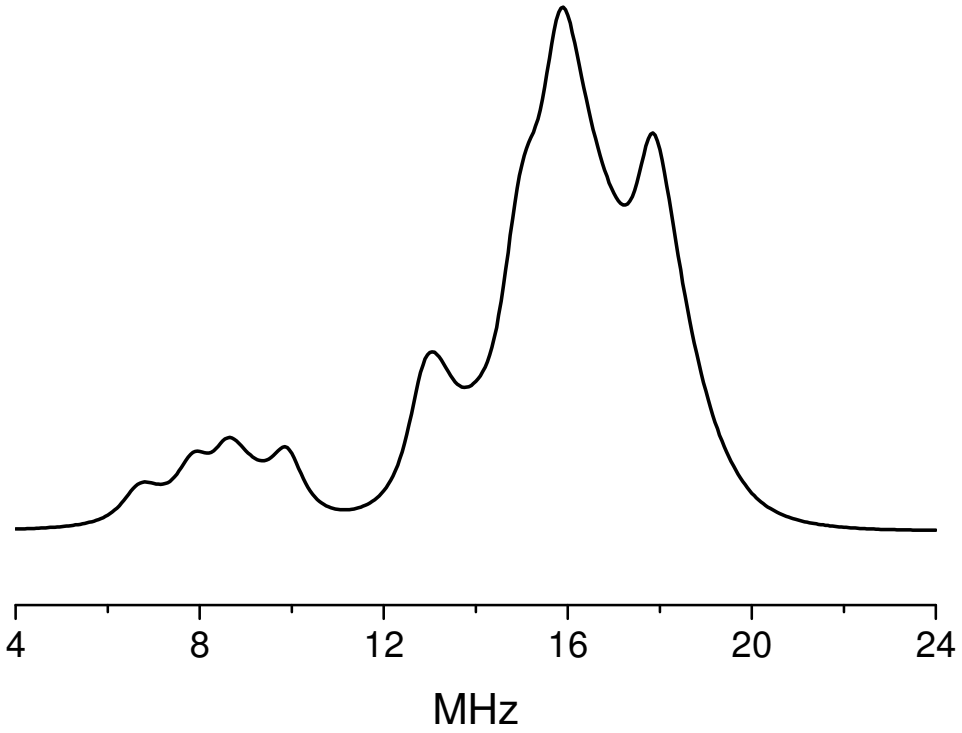

Fig. EX1C. Simulated powder ENDOR spectrum (in absorption) of ^{14}NO-ligated ferrocytochrome c heme a3, at the field setting (g = 2.079) in the X-band ESR spectrum (ν = 9.32 GHz), using ENDORF2, see LoBrutto R, Wei YH, Mascarenhas R, Scholes CP, King TE (1983) J Biol Chem 258:7437-7448 for experimental spectrum. The simulation employed a line width of 0.6 mT in weight function *s* (Gaussian shape) and a line width of 0.6 MHz in the ENDOR convolution function *t* (Lorentzian shape) using spin Hamiltonian parameters in example file EX1C.dat

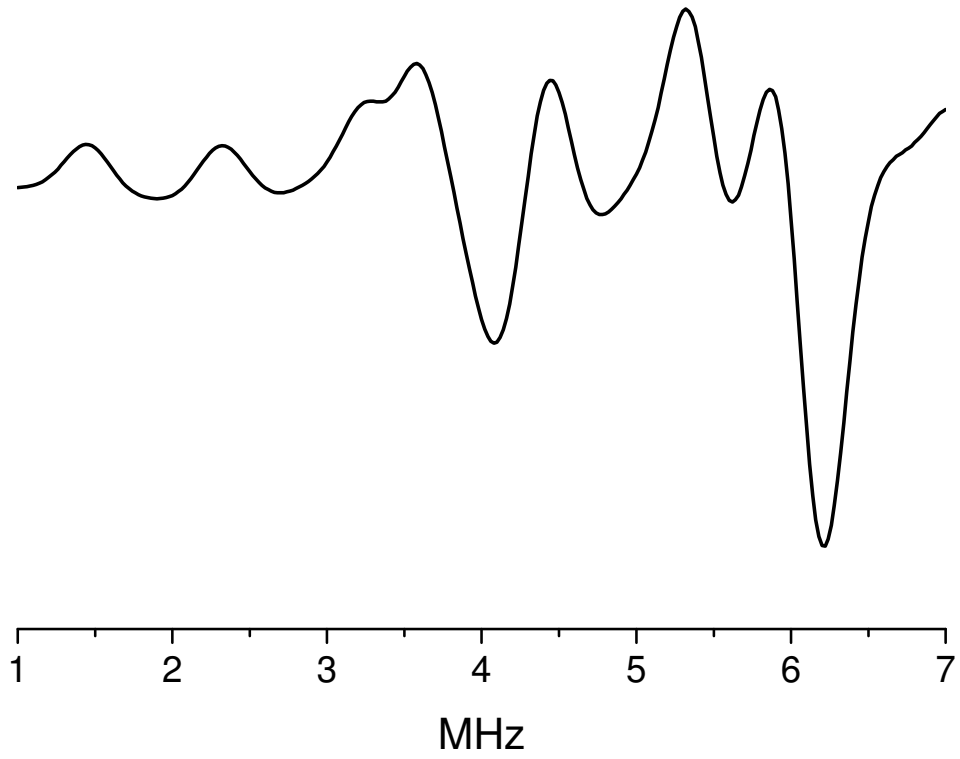

Fig. EX2H Simulated ENDOR spectra at 110 K of the $\dot{C}H_2NHCOC_6H_5$ -radical formed in X-irradiated polycrystalline hippuric acid. Only the region containing ^{14}N-signals is shown, see Erickson R (1996) Chem Phys 202:263-275 for theory and experimental spectrum. The simulation employed a Gaussian line width of 0.1 mT in weight function *s* and a Lorentzian convolution function *t* with line width 0.6 MHz, using spin Hamiltonian parameters in example file EX2_H.dat

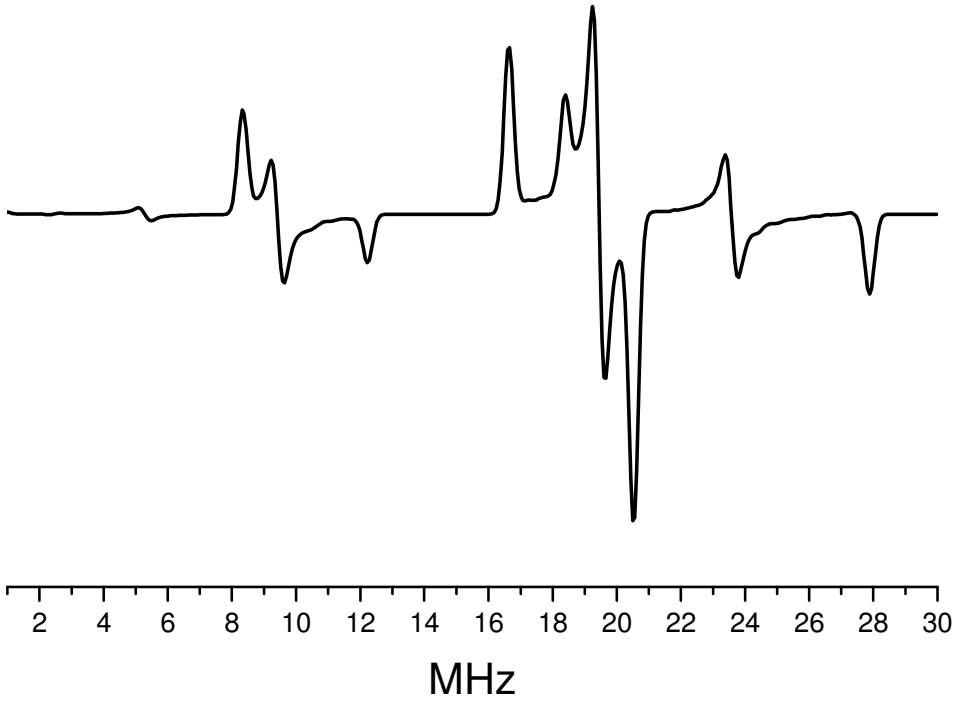

Fig. EX3B. Simulated powder ENDOR spectra of the biphenyl radical cation in $CFCl_3$ matrix at 120 K, see Erickson R (1996) Chem Phys 202:263-275 for theory and experimental spectrum. The spectrum was calculated using the spin Hamiltonian parameters in input example file EX3B.dat, at magnetic field B = 341.40 mT and microwave frequency ν = 9.5670 GHz. The simulation included *para*- and *ortho*-protons but matrix fluorine and *meta* protons were excluded in the simulations. The weight function *s* and convolution function *t* had line widths of 0.1 mT, and 0.3 MHz (both Gaussian shaped)

ENDORF2 INPUT

INPUT TO THE PROGRAM IS PROVIDED FROM AN INPUT FILE.THE PROGRAM
STARTS BY ASKING IF YOU WANT TO CREATE A FILE OR NOT. IF THE
FILE EXISTS TYPE 'N' AND THEN GIVE THE DATAFILE NAME. TO INSTEAD
CREATE A FILE TYPE 'Y' AND ANSWER THE QUESTIONS GIVEN BY THE
PROGRAM. MULTIPLE CASES MAY BE GIVEN IN THE SAME FILE. WHEN YOU
HAVE GIVEN THE DATA SAVE THE FILE BY TYPING **** AT THE
QUESTION 'Comment(Stop with ****):'.EXECUTION OF THE PROGRAM IS
THEN HALTED. TO RUN THE SIMULATION RESTART THE PROGRAM AND GIVE
THE FILENAME.
At most 10 characters are allowed for file names

ALL FORMATS ARE FREE, IF NOT STATED OTHERWISE

#	DESCRIPTION	FORMAT
1	text=TEXT FOR IDENTIFICATION	(18A4)
2	INUM,SECO INUM= NUMBER OF SETS OF NUCLEI. ALL NUCLEI WITH THE SAME SPIN-VALUE CONSTITUTE ONE SET SECO=1,SECOND ORDER CORRECTIONS ARE CALCULATED =0,WITHOUT SECOND ORDER CORRECTIONS	
3	LIM,LIZ,LAC,LS LIM=0 ISOTROPY LIM=1 AXIAL SYMMETRY LIM=2 NO SYMMETRY LIZ=0 POLYCRYSTAL RANDOM ORIENTATION LIZ=-4 SINGLE CRYSTAL ONE OR MORE SITES LAC=0 NO MOLECULAR SYMMETRY LAC=1 THE TENSORS HAVE ONE AXIS IN COMMON LAC=2 THE TENSORS HAVE TWO AXES IN COMMON LAC=N N-FOLD ODD SYMMETRY AXIS LAC=-N N-FOLD EVEN SYMMETRY AXIS LS=0 NON-EQUIVALENCE OF ALL NUCLEI LS=1 EQUIVALENCE OF SOME OR ALL NUCLEI	
4	SET OF DATA FOR INTEGRATION,AS IN PROGRAM MARU	
	(LIZ=0) Polycrystal	
4A	NU,NI: NU*NI=HALF THE NUMBER OF ANGLES THETA OF STATIC FIELD (LIM=2) 4A REPEATED FOR ANGLES FI	
	(LIZ=-4) SINGLE CRYSTAL	
4A	NUMBER OF SITES. IN THIS VERSION ONLY ONE SITE IS ALLOWED	
4B	WEIGHTS OF SITES	
4	ANGLE THETA OF STATIC FIELD	
4D	ANGLE FI OF STATIC FIELD	
(4C,4D IN PAIRS AS MANY AS THERE ARE SITES)		
4E	ANGLE THETA OF RF-FIELD	
4F	ANGLE FI OF RF-FIELD NOTE THAT THE RF-FIELD MUST BE PERPENDICULAR TO THE STATIC FIELD!!!!	
5	FREQ=MICROVAVE FREQUENCY(MHZ)	
6	G-TENSOR,ONE ReCORD FOR EACH PRINCIPAL value I: G0(I)=PRINCIPAL VALUE, RG(I,J)=DIRECTION COSINES, I=1:3 3 RECORDS TO SPECIFY TENSOR	
	SETS 7-11 REPEATED INUM TIMES	
7	FIS(NUM)=NUCLEAR SPIN	

```
 8   NEQN(NUM)=NUMBER OF NUCLEI WITH SPIN FIS(NUM)

     SETS 9 AND 10 REPEATED NEQN TIMES

 9   GNN(I)=NUCLEAR G-FACTOR,
     ENHANCE(I)=ENDOR-LINE PLOT INTENSITY FACTOR
     ENHANCE(I)=1 NORMAL MODE
     ENHANCE(I)=0 INTENSITY SET TO ZERO
     VALUES OUTSIDE 0 AND 1 ARE ALLOWED BUT NOT RECOMENDED. IN
     THIS CASE CALCULATED ENDOR INTENSITIES OF THIS NUCLEUS ARE
     MULTIPLIED BY THE FACTOR ENHANCE(I).


10   hfs-TENSOR, ,ONE ReCORD FOR EACH PRINCIPAL value I:
     C0(I)=PRINCIPAL VALUE, RC(I,J)=DIRECTION COSINES, I=1:3
     3 RECORDS TO SPECIFY TENSOR

     For FIS(NUM)>½ only:
11   nqc-TENSOR, ,ONE ReCORD FOR EACH PRINCIPAL value I:
     q0(I)=PRINCIPAL VALUE, RQ(I,J)=DIRECTION COSINES, I=1:3
     3 RECORDS TO SPECIFY TENSOR


12   LG,DB,SECOND,RESOLV,SUPP
     LG=1  GAUSSIAN LINESHAPE
     LG=O  LORENTZIAN LINESHAPE
     LG=-1 NUMERICAL LINESHAPE
     DB=LINE WIDTH PEAK-PEAK DERIVATIVE
     SECOND=DERIVATIVE OF SPECIFIED SHAPE IS TAKEN
     RESOLV=LINES SEPARATED < RESOLV  ARE ADDED
     SUPP=INTENSITIES < SUPP ARE NEGLECTED
     (RESOLV AND SUPP VALUES ARE NEGLECTED IN THIS VERSION)

13   Fmin,STEP,Fmax
     Fmin=START frequency (MHz)
     STEP=STEP IN INCREMENTS OF STEP (MHz)
     Fmax=STOP frequency (MHz)


     THE PROPER VALUES OF SETS 14-16 ARE AUTOMATICALLY DEFINED
     WHEN AN INPUT FILE IS GENERATED WITH THIS PROGRAM.
     THESE SETS ARE NOT OF INTEREST FOR AN ORDINARY USER
     BUT MUST BE PRESENT IN ALL INPUT FILES.THE SETS ARE KEPT FOR
     BACKWARD COMPATIBILITY WITH OTHER PROGRAMS USED IN OUR LAB.

14   LADD,PROC,NOPLOT,PRINT,PUNCH
     LADD=0 ISOLATED
     LADD=1 START ADD SPECTRA
     LADD=2 CONTINUE ADD
     LADD=3 STOP ADD
     PROC=FRACTION OF SPECTRUM ADDED
     NOPLOT=T NO PLOT
     PRINT=T  PRINT SPECTRUM
     PUNCH=T  PUNCH SPECTRUM

     IF PLOT OF SPECTRUM,SETS 15,16

15   SWEEP,HEIGHT   (LADD.LE.1)
     SWEEP=G/CM
     HEIGHT=CM

16   TITLE   (LADD.LE.1) (8A10)
     TEXT ON PLOT

17   **** in column 1-4 STOPS INPUT
```

****

Input example 1, Fe-Cytokrom c:

```
 Fe-cytokrom
           2           0
           2           0           0           0
   24    1
   24    1
     9320.000000
       2.082000       1.000000        .000000        .000000
       1.979000        .000000       1.000000        .000000
       2.008000        .000000        .000000       1.000000
          1.0
          1
        .404000       1.000000
      16.500000       1.000000        .000000        .000000
      16.100000        .000000       1.000000        .000000
      19.300000        .000000        .000000       1.000000
        .450000       1.000000        .000000        .000000
        .670000        .000000       1.000000        .000000
      -1.120000        .000000        .000000       1.000000
          1.0
          1
        .404000       1.000000
      30.560000       1.000000        .000000        .000000
      30.560000        .000000        .953700        .300700
      59.900000        .000000       -.300700        .953700
       1.030000       1.000000        .000000        .000000
       -.510000        .000000       1.000000        .000000
       -.520000        .000000        .000000       1.000000
          1           6.000000   0    .000000        .000000
          0            .500000   0    .000000        .000000
    3202.940000       4.000000        .050000      24.000000
          0           1.000000 F F F
       1.000000       1.000000
 Fe-cytokrom                                                                *END*
****
```

Screen input to run program with previously stored file (EX1C.dat):

```
Prepare input file(Y/N):N
Input file name:EX1C.DAT
Analytical or Numerical diagonalization(A/N):A
```

Remark 1: 'N' applies generally and must be used for nuclear spin I>3/2
Remark 2: At most 10 characters are allowed for file names

Screen output when program runs:

```
Theta and Phi orientation no: (for integration of powder spectra)
Stop - Program terminated
```

OUTPUT FILES
****

THE PROGRAM GENERATES TWO OUTPUT FILES. THE FILE 'SPECTDAT' CONTAINS A SUMMARY OF THE INPUT AND ANY WARNINGS OR ERRORS ENCOUNTERED DURING EXECUTION. THE SIMULATED SPECTRUM IS STORED IN X,Y FORMAT ON A FILE 'filename#.PLT' WHERE 'filename' IS THE SAME AS THE NAME OF THE INPUT FILE AND # IS A TWO DIGIT SERIAL NUMBER 01-24 GENERATED BY THE PROGRAM.

Output example 1, Fe-Cytokrom c in file 'spectdat':

```
Fe-cytokrom
  2 SETS OF NUCLEI
```

```
 INTEGRATION Parameters
    2    0    0   48   48
 MICROWAVE FREQUENCY= 9320.0 MHz


 G-TENSOR
        2.08200        1.00000         .00000         .00000
        1.97900         .00000        1.00000         .00000
        2.00800         .00000         .00000        1.00000


    1 NUCLEI WITH I=  1.0
 A-TENSOR   GN=  .40400   Plot-intensity factor= 1.00000
       16.50000        1.00000         .00000         .00000
       16.10000         .00000        1.00000         .00000
       19.30000         .00000         .00000        1.00000
 Q-TENSOR
         .45000        1.00000         .00000         .00000
         .67000         .00000        1.00000         .00000
       -1.12000         .00000         .00000        1.00000


    1 NUCLEI WITH I=  1.0
 A-TENSOR   GN=  .40400   Plot-intensity factor= 1.00000
       30.56000        1.00000         .00000         .00000
       30.56000         .00000         .95372         .30071
       59.90000         .00000        -.30071         .95372
 Q-TENSOR
        1.03000        1.00000         .00000         .00000
        -.51000         .00000        1.00000         .00000
        -.52000         .00000         .00000        1.00000



   ESR line shape, units in (G)
 LINES  SEPARATED.LT.     .000E+00 ARE ADDED
 LINE INTENSITIES.LT.     .000E+00 ARE NEGLECTED
 LINE WIDTH              6.000
 GAUSSFORM
 INTEGRAL OF SPECIFIED LINE SHAPE TAKEN



   NMR line shape, units in (MHz)
 LINES  SEPARATED.LT.     .000E+00 ARE ADDED
 LINE INTENSITIES.LT.     .000E+00 ARE NEGLECTED
 LINE WIDTH               .500
 LORENTZFORM
 INTEGRAL OF SPECIFIED LINE SHAPE TAKEN


 START frequency     4.000  MHz  STEP   .050 MHz   401 points
 Magnetic field at   3202.940 G
 LADD=  0 PROC=   1.00000
 Spectrum written to file:ex1c01.plt

Time=     .28 seconds

Output of spectrum is in xy file 'EX1C01.PLT'
Software for  plotting  must be obtained separately

Input example 2, Irradiated powder of hippuric acid:


hippuric acid radical
          2          0
          2          0          0          0
   48    1
```

```
  48    1
    9573.700000
      2.002800       1.000000        .000000        .000000
      2.002800        .000000       1.000000        .000000
      2.002800        .000000        .000000       1.000000
          .5
           2
      5.585000       1.000000
    -24.220000       -.496000        .792000        .357000
    -48.700000        .072000       -.372000        .926000
    -81.200000        .866000        .484000        .128000
      5.585000       1.000000
    -25.460000       -.413000       -.847000       -.334000
    -48.980000        .081000       -.400000        .913000
    -79.060000       -.908000        .350000        .234000
         1.0
           1
       .404000       1.000000
      -7.580000        .185000       -.432000        .883000
      -8.470000        .983000        .057000       -.178000
      -9.440000        .027000        .900000        .435000
       -.843000        .195000       -.398000        .896000
        .582000        .980000        .128000       -.157000
        .261000       -.050000        .909000        .415000
          1           1.000000   0    .000000        .000000
          1            .300000   1    .000000        .000000
   3415.300000       1.000000         .020000       7.000000
          0          1.000000 F F F
      1.000000       1.000000
 hippuric acid radical                                                  *END*
****
```

Output example 2, Irradiated powder of hippuric acid:

```
hippuric acid radical
  2 SETS OF NUCLEI


 INTEGRATION Parameters
    2    0    0   96   96
 MICROWAVE FREQUENCY= 9573.7 MHz


 G-TENSOR
        2.00280        1.00000         .00000         .00000
        2.00280         .00000        1.00000         .00000
        2.00280         .00000         .00000        1.00000


    2 NUCLEI WITH I=   .5
 A-TENSOR   GN= 5.58500   Plot-intensity factor= 1.00000
      -24.22000        -.49582         .79171         .35687
      -48.70000         .07196        -.37181         .92552
      -81.20000         .86574         .48386         .12796
 A-TENSOR   GN= 5.58500   Plot-intensity factor= 1.00000
      -25.46000        -.41310        -.84720        -.33408
      -48.98000         .08099        -.39997         .91294
      -79.06000        -.90722         .34970         .23380


    1 NUCLEI WITH I=  1.0
 A-TENSOR   GN=  .40400   Plot-intensity factor= 1.00000
       -7.58000         .18495        -.43188         .88276
       -8.47000         .98240         .05697        -.17789
       -9.44000         .02700         .90002         .43501
 Q-TENSOR
        -.84300         .19507        -.39815         .89634
         .58200         .97930         .12791        -.15689
```

```
         .26100        -.04997         .90854         .41479


   ESR line shape, units in (G)
 LINES  SEPARATED.LT.     .000E+00 ARE ADDED
 LINE INTENSITIES.LT.     .000E+00 ARE NEGLECTED
 LINE WIDTH              1.000
 GAUSSFORM
 INTEGRAL OF SPECIFIED LINE SHAPE TAKEN



   NMR line shape, units in (MHz)
 LINES  SEPARATED.LT.     .000E+00 ARE ADDED
 LINE INTENSITIES.LT.     .000E+00 ARE NEGLECTED
 LINE WIDTH               .300
 GAUSSFORM


 START frequency     1.000  MHz  STEP   .020 MHz   301 points
 Magnetic field at   3415.300 G
 LADD=  0 PROC=   1.00000
 Spectrum written to file:ex2h01.plt

Time=    2.17 seconds


Input example 3, Irradiated biphenyl in frozen solution:


bifenyl cation ENDOR
           3           0
           2           0           1           0
   48    3
   48    2
     9567.000000
       2.003000       1.000000        .000000        .000000
       2.002100        .000000       1.000000        .000000
       2.002200        .000000        .000000       1.000000
            .5
             2
       5.585000       1.000000
     -26.900000       1.000000        .000000        .000000
      -7.900000        .000000       1.000000        .000000
     -18.300000        .000000        .000000       1.000000
            5.585000       1.000000
     -26.900000       1.000000        .000000        .000000
      -7.900000        .000000       1.000000        .000000
     -18.300000        .000000        .000000       1.000000
            .5
             2
       5.585000       1.000000
     -12.200000        .377100        .926200        .000000
      -4.400000        .926200       -.377100        .000000
     -10.000000        .000000        .000000       1.000000
            5.585000       1.000000
     -12.200000        .377100        .926200        .000000
      -4.400000        .926200       -.377100        .000000
     -10.000000        .000000        .000000       1.000000
            .5
             2
       5.585000       1.000000
     -12.200000       -.377100        .926200        .000000
      -4.400000        .926200        .377100        .000000
     -10.000000        .000000        .000000       1.000000
       5.585000       1.000000
     -12.200000       -.377100        .926200        .000000
      -4.400000        .926200        .377100        .000000
     -10.000000        .000000        .000000       1.000000
```

```
         1            1.000000   0    .000000        .000000
         1             .300000   1    .000000        .000000
    3410.000000       1.000000        .060000      30.000000
         0            1.000000 F F F
       1.000000       1.000000
 bifenyl cation ENDOR                                                    *END*
****
```

Output example 3, Irradiated biphenyl in frozen solution:

```
bifenyl cation ENDOR
  3 SETS OF NUCLEI


 INTEGRATION Parameters
    2    0    1  288  192
 MICROWAVE FREQUENCY= 9567.0 MHZ


 G-TENSOR
        2.00300        1.00000         .00000         .00000
        2.00210         .00000        1.00000         .00000
        2.00220         .00000         .00000        1.00000


    2 NUCLEI WITH I=   .5
 A-TENSOR   GN= 5.58500   Plot-intensity factor= 1.00000
      -26.90000        1.00000         .00000         .00000
       -7.90000         .00000        1.00000         .00000
      -18.30000         .00000         .00000        1.00000
 A-TENSOR   GN= 5.58500   Plot-intensity factor= 1.00000
      -26.90000        1.00000         .00000         .00000
       -7.90000         .00000        1.00000         .00000
      -18.30000         .00000         .00000        1.00000


    2 NUCLEI WITH I=   .5
 A-TENSOR   GN= 5.58500   Plot-intensity factor= 1.00000
      -12.20000         .37710         .92620         .00000
       -4.40000         .92620        -.37710         .00000
      -10.00000         .00000         .00000        1.00000
 A-TENSOR   GN= 5.58500   Plot-intensity factor= 1.00000
      -12.20000         .37710         .92620         .00000
       -4.40000         .92620        -.37710         .00000
      -10.00000         .00000         .00000        1.00000


    2 NUCLEI WITH I=   .5
 A-TENSOR   GN= 5.58500   Plot-intensity factor= 1.00000
      -12.20000        -.37710         .92620         .00000
       -4.40000         .92620         .37710         .00000
      -10.00000         .00000         .00000        1.00000
 A-TENSOR   GN= 5.58500   Plot-intensity factor= 1.00000
      -12.20000        -.37710         .92620         .00000
       -4.40000         .92620         .37710         .00000
      -10.00000         .00000         .00000        1.00000



   ESR line shape, units in (G)
 LINES  SEPARATED.LT.     .000E+00 ARE ADDED
 LINE INTENSITIES.LT.     .000E+00 ARE NEGLECTED
 LINE WIDTH              1.000
 GAUSSFORM
 INTEGRAL OF SPECIFIED LINE SHAPE TAKEN
```

```
   NMR line shape, units in (MHz)
 LINES  SEPARATED.LT.      .000E+00 ARE ADDED
 LINE INTENSITIES.LT.      .000E+00 ARE NEGLECTED
 LINE WIDTH                .300
 GAUSSFORM


 START frequency     1.000  MHz  STEP   .060 MHz   484 points
 Magnetic field at   3410.000 G
 LADD=  0 PROC=   1.00000
 Spectrum written to file:ex3b01.plt

Time=  538.23 seconds
```

Paper 5

Simulation of ENDOR spectra of radicals with anisotropic hyperfine and nuclear quadrupolar interaction in disordered solids

Reprint from "Electron Magnetic Resonance of Free Radicals. Theoretical and Experimental EPR, ENDOR and ESEEM Studies of Radicals in Single Crystal and Disordered Solids", Roland Erickson, PhD Thesis No 391, Linköping University, 1995.

Simulation of ENDOR spectra of radicals with anisotropic hyperfine and nuclear quadrupolar interactions in disordered solids.

Roland Erickson

Chemical Physics Laboratory, Department of Physics and Measurement Technology, IFM/FOA, Linköping University, S-581 83 Linköping, Sweden

Abstract

A general theory to calculate ENDOR spectra of S=1/2 radicals in single crystal or disordered solids is presented. The theory is suitable for paramagnetic systems with n interacting nuclei which can be described by the spin-Hamiltonian $\mathcal{H} = \beta \mathbf{B}\mathbf{g}\mathbf{S} + \sum_{i=1}^{n} \mathbf{I}_i \mathbf{A}_i \mathbf{S} + \mathbf{I}_i \mathbf{Q}_i \mathbf{I}_i - g_i \beta_N \mathbf{B}\mathbf{I}_i$. There are no restrictions on the relative magnitude of the hyperfine, quadrupolar and nuclear Zeeman interactions, nor on the relative orientation of principal axes of the tensors. ENDOR transition frequencies and intensities are calculated with perturbation theory under the assumption that the electron Zeeman interaction is dominating. A simple formula for first order transition moments, including the effect of the quadrupolar coupling, is presented. The impact on the transition moment of the orientational distribution of the radio-frequency field in single crystal and disordered systems is taken into account. The method is tested against experimental proton- and ^{14}N-ENDOR data of neutral and ionic radicals in disordered solids.

1. Introduction

The hyperfine and quadrupolar interactions in radical species provide probes of the electronic and geometrical structure of the system. The interactions can be characterized by conventional electron spin resonance (EPR, ESR), or with enhanced resolution by electron-nuclear double resonance (ENDOR). The resolution of EPR is often sufficient for species in solution or single crystal samples. But for radicals that can only be prepared in disordered solids the limited resolution of EPR may be inadequate. By disordered solids we mean glassy, polycrystalline, frozen solution or amorphous samples, which we will refer to as powders. In powder EPR the spectral interpretation is often hampered due to g, hyperfine and quadrupolar anisotropy in combination with inhomogeneous line broadening. The resolution is further diminished if the electron interacts with several nuclei as the number of EPR transitions increases multiplicatively with the number of nuclei. ENDOR has higher resolution and the complexity of the spectrum can be reduced since the number of ENDOR transitions increases additively instead of multiplicatively. Radical species investigated by powder ENDOR include organic radical ions on catalytic surfaces [1-4] and in frozen matrices [3,5-8], organic radicals trapped in molecular crystals [9], as well as radical systems of biological interest [10,11].

However powder ENDOR spectra are often not as straightforward to interpret as spectra in solution or single crystals. Powder lines are usually broader and the anisotropy of hyperfine and quadrupolar interactions can produce complex lineshapes in the powder spectrum. Computer simulation of the spectrum can greatly aid an accurate assignment of spectroscopic parameters. Clarkson et al have used a theory, originally due to Dalton and Kwiram [9], to analyse powder ^{1}H-ENDOR of perylene$\cdot^+$ generated on silica-alumina catalysts.[1] The method is based on perturbation theory where transition moments are calculated to first order and relaxation effects are taken into account. Kispert and co-workers have used simulation methods to analyse ^{1}H-ENDOR spectra from carotenoid cation radicals stabilized on Nafion films and silica gel [2].

Powder ENDOR spectra are further complicated by orientational selectivity. In a powder the spectrum is a sum of contributions from a range of orientations. In general only the orientations that correspond to the EPR field setting are observed, provided the cross relaxation is not too fast. If either g or the hyperfine anisotropy is dominating single-crystal like ENDOR spectra can be obtained at g-value or hyperfine extrema (turning points) in the EPR spectrum, as first pointed out by Rist and Hyde [12]. But to determine all principal tensor values and tensor orientations it is usually required to interpret spectra obtained at intermediate field positions. Hoffman [13,14], Henderson [15], Yordanov [16] and their co-workers have shown that useful information can be obtained through computer simulation of the ENDOR signals acquired across the EPR spectrum. Orientational selectivity was taken into account but transition moments were not computed. EPR lines of finite linewidth were used by Hoffman and co-workers [13,14] in the orientational selection instead of the common approximation of δ-function EPR lineshapes. A general theory to calculate powder ENDOR spectra due to arbitrary zero-field splitting, hyperfine and quadrupolar interactions has been described by Kreiter and Hüttermann [17]. Exact diagonalization of the spin Hamiltonian was employed to calculate magnetic energies and wave functions. The ENDOR transition moments were calculated to zeroth order, neglecting hyperfine enhancement effects. A similar theory has been described by Keijzers et al [18].

In this report we present a method to calculate single crystal or powder ENDOR spectra of S=1/2 radicals with hyperfine and quadrupolar interactions. ENDOR transition moments and frequencies are calculated using perturbation theory. No restrictions are imposed on the quadrupolar, nuclear Zeeman and hyperfine interactions other than that they must be much smaller than electron Zeeman interaction. ENDOR transition moments are computed to first order. First order formulas given previously [19,20] exclude quadrupolar interactions. The impact of the RF-field orientation on the transition moment in powders is taken into account with analytical integration. ENDOR frequencies are calculated neglecting second order hyperfine contributions in blocks offdiagonal with respect to electron spin. The theory differs from the usual perturbation schemes for multiple nuclei (see for example Ref. 21) in that quadrupolar couplings of the same order as the hyperfine coupling can be treated. The treatment is particularly suitable for simulation of powder spectra with several magnetic nuclei where the exact theory may result in slow calculations [17,18]. The theory is tested against experimental ^{14}N- and ^{1}H-ENDOR of radicals with and without quadrupolar interactions present.

2. Experimental

Biphenyl-h_{10} (Ph_2), (99%) and hippuric acid (98%) , $C_6H_5CONHCH_2CO_2H$, were obtained commercially (Aldrich) and used without further purification. Sample preparation of biphenyl samples has been described previously [3]. Polycrystalline hippuric acid was irradiated at room temperature for 30 min with a Philips X-ray tube operating at 20 mA and 70 kV. The irradiated powder was placed in a Suprasil quartz sample tube and measured at 110 K. EPR and ENDOR measurements were performed on a Bruker ER200D-SRC spectrometer equipped with an ER250 ENDOR accessory and a EIN AF-500 RF-amplifier. ENDOR spectra were obtained using a RF modulation depth of 111 to 200 kHz.

3. Theoretical method

3.1 Perturbation treatment of the spin Hamiltonian

The theory used for ENDOR spectra simulation is based on a perturbation treatment of the spin Hamiltonian:

$$\mathcal{H} = \beta \mathbf{B} \mathbf{g} \mathbf{S} + \sum_{i=1}^{n} \mathbf{I}_i \mathbf{A}_i \mathbf{S} + \mathbf{I}_i \mathbf{Q}_i \mathbf{I}_i - g_i \beta_N \mathbf{B} \mathbf{I}_i \ , \qquad (1)$$

where the summation is over n nuclei and S=1/2 is assumed. The first term, the electron Zeeman interaction, is assumed to be dominating. Terms $\mathbf{g}$, $\mathbf{A}_i$, and $\mathbf{Q}_i$ are the g, hyperfine, and quadrupole coupling tensors, and g_i is the g-factor of nucleus i. There are no restrictions on the relative magnitude of the hyperfine, quadrupolar and nuclear Zeeman interactions, nor on the relative orientation of principal axes of the tensors. The nuclear Zeeman interactions are assumed to be isotropic. The theory to calculate ENDOR transition frequencies and transition intensities is an extension of a theory for EPR simulation described previously [22,23]. The theory has shown good performance [22] in analysing EPR spectra of organic radicals as well as halogen containing radicals such as $\cdot S_2Cl$ where the quadrupolar interaction can be as large as the hyperfine coupling.

The tensors are expressed in an arbitrary laboratory co-ordinate system in which the static field **B** with strength B is directed along the unit vector ℓ=**B**/B. By introducing the mutually orthogonal unit vectors **p**, **q**, and **u**, where **u** = gℓ/g is the effective Zeeman field direction, the Hamiltonian (1) can be rewritten as:

$$\mathcal{H} = \mathcal{H}^{eZ} + \sum_{i=1}^{n} \mathcal{H}_i' + \mathcal{H}_i'' \tag{2}$$

$$\mathcal{H}^{eZ} = g\beta B S_u \tag{3}$$

$$\mathcal{H}_i' = \mathbf{I}_i \mathsf{A}_i \mathbf{u} S_u + \mathbf{I}_i \mathsf{Q}_i \mathbf{I}_i - g_i \beta_N B \ell \mathbf{I}_i . \tag{4}$$

$$\mathcal{H}_i'' = (\mathbf{I}_i \mathsf{A}_i \mathbf{p}) S_p + (\mathbf{I}_i \mathsf{A}_i \mathbf{q}) S_q \tag{5}$$

The g-factor is given by $g^2 = \ell g^2 \ell$. The terms S_p, S_q and S_u are the components of **S** along the **p**, **q**, and **u** vectors. The term $\Sigma\, \mathcal{H}_i''$ can be treated as a perturbation if the electron Zeeman term (3) is dominating [24]. Exact diagonalization of $\mathcal{H}^{eZ} + \sum \mathcal{H}_i'$ using the basis $\Psi(M_S, m_1, m_2, \ldots m_n) = \phi(M_S)\phi(m_1)\phi(m_2)\ldots\phi(m_n)$ is done by a procedure described previously [22,23]. There are no matrix elements between $M_S = \pm ½$ and the matrix is block diagonal with respect to each nucleus. It is thus sufficient to diagonalize $\mathcal{H}_i'$ separately for each nucleus i and M_S-value. In contrast to diagonalization of the full Hamiltonian, $\mathcal{H}$, the matrices will be small, dimension $(2I+1)$ x $(2I+1)$ for a nucleus of spin I. General, analytical formulas for the nuclear eigenenergies and eigenstates have been derived for I=1 and I=3/2 [23]. Nuclei with I ≥ 2 require numerical diagonalization. Matrix elements of $\mathcal{H}_i'$ are listed in Refs. 22 and 23. The obtained nuclear eigenstates for the two M_S-values, ±½, are linear combinations of nuclear spin states:

$$|v_i> = \sum_{m_i=-I_i}^{I_i} \gamma_{v_i,m_i} |\phi(m_i)\rangle, \qquad v_i = 1, 2, \ldots, 2I_i+1 \quad , M_S = +1/2 \tag{6a}$$

$$|w_i> = \sum_{m_i=-I_i}^{I_i} \lambda_{w_i,m_i} |\phi(m_i)\rangle, \qquad w_i = 1, 2, \ldots, 2I_i+1 \quad , M_S = -1/2 \tag{6b}$$

The corresponding energies are denoted by E_{v_i} and E_{w_i} respectively. The full eigenfunction is given by $|+½, v_1, \ldots, v_n> = |+½>|v_1>|v_2>\ldots|v_n>$ with the corresponding energy $+½g\beta B + \sum_i E_{v_i}$. The expressions for states in the -½ -manifold are analogous. The first order eigenfunctions for $M_S = +½$ are given by:

$$|\Phi(+½, v_1, ..., v_n)> = |+½, v_1, ..., v_n> +$$

$$\sum_{w_1 w_2 .. w_n} \frac{\langle -½, w_1, ..., w_n | \sum_{i=1}^{n} \mathcal{H}_i'' | +½, v_1, ..., v_n \rangle}{+g\beta B} | -½, w_1, ..., w_m \rangle , \qquad (7)$$

where the outer summations runs over all nuclear states $|w_i>$ in $|-½, w_1, ..., w_n> = |-½>|w_1> |w_2>...|w_n>$. The labels in $\Phi(+½, v_1, ..., v_n)$ identify the state labels of the leading term in the first order expression. Energy terms smaller than the order of $g\beta B \times 10^{-2}$, caused by the nuclear interactions $\mathcal{H}_i''$, have been neglected in the denominator. The corresponding expression for $|\Phi(-½, w_1, w_2, ..., w_n)>$ is obtained by exchanging places of all v_i and w_i, and plus and minus signs in formula (7).

3.2 ENDOR transition frequencies

The perturbation (5) gives no energy contribution to first order, with respect to electron spin, and the ENDOR transition frequency between two nuclear eigenstates $|a_i>$ and $|b_i>$, $\Delta M_s = 0$, is obtained as:

$$f_{a_i b_i} = | E_{a_i} - E_{b_i} |, \qquad (8)$$

where $|a_i>$ and $|b_i>$ belong to the same M_s-manifold, i.e. either the $|v_i>$ or the $|w_i>$-manifolds defined in Eq. (6a-b). Note that in general the eigenstates are mixtures of nuclear spinstates (cf. Eq. (6)). Analytical (I<2) and numerical (I≥2) methods to compute the energies and wavefunctions have been described [22,23].

3.3 ENDOR transition moments in single crystals

In a single crystal the square of the ENDOR transition moment is given to first order by:

$$W^2 = (\frac{B_2}{B})^2 | < a_i | \mathbf{I}_i \cdot \mathbf{C}_i \cdot \mathbf{r} | b_i > |^2 , \qquad (9)$$

where

$$\mathbf{C}_i = M_s \mathbf{A}_i \mathbf{g} / g - \nu_i \mathbf{1} , \qquad (10)$$

and $\mathbf{1}$ is the identity matrix and ν_i is the nuclear Larmor frequency[#1] . The terms B_2 and $\mathbf{r}$ are the strength and direction of the RF-field $\mathbf{B}_2$, which is oriented perpendicular to the static field direction ℓ. Transition moments in powders are discussed further below. Equations (9)-(10) are valid for $\frac{1}{g^2} \mathbf{r} \mathbf{g}^2 \ell << 1$, i.e. for modest g-anisotropy and $\mathbf{r}$ orthogonal to ℓ. For very small g-anisotropy the factor $\mathbf{g}/g$ in Eq. (10) will have negligible effect on W^2 and can be replaced by the identity matrix $\mathbf{1}$. Each nucleus with nonzero nqi gives rise to $(2I+1)^2$ EPR transitions and

[#1] A few misprints have been discovered in the corresponding formulas in section 3 of Ref. [3], i.e. paper 4 of this thesis. These have been corrected in the reprint of paper 4 in this thesis.

$2I(2I+1)$ ENDOR transitions. ENDOR transitions between all nuclear spin states within the same M_S-manifold of a nucleus are more or less allowed. Similarly EPR transitions between all initial and final nuclear spin states with different M_S-value are allowed. With zero nqi the number of ENDOR transitions reduces to $4I$ with the selection rule $\Delta M_S = 0$, $\Delta m_I = \pm 1$. Here m_I is the quantum number of the nuclear spin operator $\mathbf{I}_k$ along the nuclear quantization axis given by $\mathbf{k} = \mathbf{C}\cdot\boldsymbol{\ell} \,/\, |\, \mathbf{C}\cdot\boldsymbol{\ell}\,|$.

Eq. (9) is derived from the general expression for the squared transition moment:

$$W^2 = |\langle \Phi(M_S, \underline{a}, a_i)|\, \mathbf{B}_2\cdot(\beta \mathbf{g}\mathbf{S} - \sum_{i=1}^{n} g_i\beta_N \mathbf{I}_i)\,|\, \Phi(M_S, \underline{a}, b_i)\rangle|^2 \,, \qquad (11)$$

using the first order wave functions (7). The label $\underline{a}$ is an abbreviation for the states $a_1,\ldots, a_{i-1}, a_{i+1},\ldots, a_n$. of the nuclei which remain unchanged in the transition. The derivation is described in detail in the appendix.

First order contributions, often called hyperfine enhancements, are important to predict ENDOR transition moments properly. The enhancement effect can be very large for nuclei with small magnetic moments, such as ^{14}N. For nuclei with large magnetic moments such as protons the effect is less dramatic but it can still cause unexpectedly low intensities for the low frequency transition, making it difficult to detect in a powder sample. This is particularly pronounced when the hyperfine coupling is of the same order as twice the nuclear Zeeman frequency as the low frequency transition will have almost zero intensity. A theoretical discussion of hyperfine enhancement for α-protons in solids, and the importance of calculating transition moments to at least first order to predict the effect has been published by Whiffen [24]. First order expressions, neglecting nuclear quadrupolar interactions (nqi), of ENDOR transition moments in single crystals have been reported by Toriyama et al [19] and Dalton and Kwiram [9] valid for small g-anisotropy, and by Schweiger and Günthard [20] including effects of g-anisotropy. Eq. (9) differs in the respect that nqi are taken into account but for nuclei with zero nqi the expression will become equivalent to the squared transition moment given in formula (27) of the paper by Toriyama et al [19]. That formula has also been given in a different notation by Schweiger et al [20].

3.4 ENDOR transition moments in powders

The transition moment in a single crystal is, in general, anisotropic and depends on the orientation of the molecule to both the static and the RF-field [19,20,24,25]. Calculating the squared transition moment W^2 in a powder sample requires integration of W^2 over angle ψ for each set of θ and φ. Angles θ and φ are the polar co-ordinates of **B**, and the angle ψ relates the orientation of the molecule to the RF-field direction for each direction of **B**, see Fig. 1. In a powder all molecules with the same orientation with respect to **B** will have the same resonance frequency but they will have different orientations relative to $\mathbf{B}_2$. The variation in W with the orientation of $\mathbf{B}_2$ can be significant, as pointed out by several authors [20,24]. Orientational dependence is found already for zeroth order transition moments [25]. Analytical integration of Eq. (9), over the distribution of $\mathbf{B}_2$ directions in the plane perpendicular to **B** gives the expression:

$$\overline{W}^2(\theta,\varphi) = \int_{\psi} W^2(\theta,\varphi,\psi)d\psi = \tfrac{1}{2}(\frac{B_2}{B})^2(\,\alpha^*C^2\alpha - \alpha^*C\,\ell\cdot\alpha C\,\ell\,)\,, \qquad (12)$$

where α is a vector with the components $<a \mid I_x \mid b>$, $<a \mid I_y \mid b>$ and $<a \mid I_z \mid b>$ and α^* is obtained by complex conjugation of the components. The nuclear index i has been dropped for simplicity. The integral is derived in the appendix. The integration is done in a similar fashion as done by Kottis and Lefebvre [26] for the microwave field in triplet state EPR spectra. Analytical integration avoids the need for a time consuming numerical integration of W^2 over ψ.

3.5 The ENDOR powder lineshape

The first derivative powder line shape at the ENDOR frequency f and static magnetic field B is approximated by the formula:

$$\frac{d}{df}\chi(B,f) = \int_{\theta}\sin\theta\int_{\varphi}\sum_{j}\{\; s(B-B_j)V_j^2\{\;\frac{d}{df}\sum_{k}t(f-f_{jk})\overline{W}_{jk}^2\;\}\}d\varphi d\theta\,, \qquad (13)$$

where

$$\overline{W}_{jk}^2 = \int_{\psi} W_{jk}^2(\theta,\varphi,\psi)d\psi, \qquad (14)$$

The summations run over the EPR transition fields $B_j(\theta,\phi)$ and the ENDOR transition frequencies $f_{jk}(\theta,\phi)$, with the corresponding transition moments $V_j(\theta,\phi)$ and $W_{jk}(\theta,\phi,\psi)$. The calculation of B_j and V_j has been described previously [22,23]. The component EPR line shape function s acts as a weighting function. It selects the transitions that contribute to the ENDOR signal at a particular field setting. Further we assume that only nuclear transitions which have an energy level in common with the EPR transitions that are in resonance will give an ENDOR response. The function t is a convolution function describing the line shape of a specific ENDOR transition. The functions s and t can be selected as Lorentzian or Gaussian shaped. The integration over ψ is described above. Integration over θ and ϕ are performed using Gaussian quadrature as described in Ref. 27.

Eq. (13) is similar to the ENDOR lineshape function derived by Kreiter and Hüttermann [17], following the principles of powder ENDOR lineshapes given by Hoffman and coworkers[13]. However, we calculate transition moments W_{jk} to first order and take into account the dependence of W_{jk} on the RF-field direction, see Eq. (12) and (14). The intensity dependence due to g-anisotropy is neglected and we assume constant, isotropic linewidths for the lineshape functions. Neither spin relaxation nor instrumental effects on the line shape are included in Eq. (13).

It should here be noted that the orientational selectivity depends on the ratio between the electron spin-spin relaxation rate (T_{xe}^{-1}) and the electron spin-lattice relaxation rate (T_{1e}^{-1}) [9]. Orientational selectivity is efficient if $T_{xe}^{-1} << T_{1e}^{-1}$ which is the common situation for transition metal complexes and radicals in frozen solution above 77K [28]. The ENDOR spectrum is then the sum of all transitions that are connected to the EPR transitions in resonance. In the other limit, when $T_{xe}^{-1} >> T_{1e}^{-1}$, the ENDOR spectrum is the sum of all possible orientations irrespective of which part of the EPR spectrum that is monitored. This situation has been encountered for organic radicals at very low temperatures, ≤ 4 K [9,28].

This case is not implemented in Eq. (12) but has been treated for I=1/2 nuclei by Dalton and Kwiram [9].

The simulation program written in Microsoft FORTRAN is available upon request to the authors. The spectrum (Fig. 3b) from irradiated hippuric acid took approximately 12 min to calculate on a 486-PC computer. The calculation included one nitrogen and two protons (table 3) and employed 9200 orientations.

4. **Results and discussion**

We have tested the performance of the theory against two categories of powder data; ^{14}N-ENDOR with quadrupolar interactions and ^{1}H-ENDOR of α-proton hyperfine couplings.

4.1 ENDOR of nitrogen nuclei in NO-ligated ferrocytochrome c oxidase heme a_3

The accuracy of the theory was tested against data of NO-ligated ferrocytochrome *c* oxidase heme a_3. Powder ENDOR spectra obtained by LoBrutto et al [11] have been simulated by Kreiter and Hüttermann [17] employing an exact diagonalization of the spin Hamiltonian. Nitrogen ENDOR signals are detected from the histidine and NO ligands of the central ferrous ion. The calculated spectrum (absorbtion lineshape) in Fig. 2, was made with the parameters from Refs. 11 and 17, see table 1 and the figure legend. The quadrupolar couplings are small compared to the hyperfine couplings. All tensors have parallel principal directions except the A-tensor of the NO-nitrogen which is rotated 17.5° around the x-direction. The spectrum was obtained at g = 2.079, near the principal value g = 2.082. The peak positions we obtain, table 2, agree with those in the simulation by Kreiter and Hüttermann [17]. The difference in peak positions is less than 0.07 MHz. The agreement with experimental peak positions is as good as that obtained in Ref. 17. The squared transition moments are calculated by Eq. (12). This is valid to first order since the g-anisotropy fulfils the condition $\frac{1}{g^2}\mathbf{r}\mathbf{g}^2\boldsymbol{\ell} << 1$. The relative intensities of the histidine and NO-nitrogen lines are different from the simulation in Ref. 17, where transition moments are calculated to zeroth order. Zero order moments do not take into account hyperfine enhancement effects [20,24,25] which can be important for low magnetic moment nuclei such as ^{14}N.

4.2 ENDOR of nitrogen nuclei in X-irradiated hippuric acid

To further test the capability of the theory developed we have investigated the ENDOR spectrum of the $\dot{C}H_2NHCOC_6H_5$ -radical formed in polycrystalline hippuric acid, Fig. 3. Only the region of ^{14}N-signals is shown. The spectrum was obtained at 110 K in the centre of the EPR spectrum(not shown). The system has been investigated previously [29] with ENDOR in single crystal at 77K, but no powder ENDOR study is known to us. The nitrogen nucleus is characterized by a substantial quadrupolar interaction compared to the hyperfine and nuclear Zeeman interactions. The ^{14}N-parameters in table 3 were used in the two simulations in Fig. 3, including and excluding quadrupolar interaction. The nitrogen parameters are those of Ref. 29 apart from the two smaller principal hyperfine values of the nitrogen which are slightly altered to improve the fit. The interactions are too small to be studied by conventional EPR even in a single crystal. The hyperfine tensors, table 3, of the two α-protons included in the calculation are as in Ref. 29. The *g*-anisotropy is small and has been taken to be isotropic [29].

Comparison of the two simulations show that quadrupolar interaction must be included to fit observed line positions. The hyperfine tensor is fairly isotropic in character. Neglect of quadrupolar interactions produces essentially two broad ENDOR lines, not observed experimentally. Inclusion of the quadrupolar interaction gives a better fit of line positions. The lowest ENDOR line cannot be observed as the region below 2 MHz is affected by a sharp decline in baseline and other instrumental effects. In the experimental curve there is also an overlapping line at 3.6 MHz which we attribute to a proton signal. There is a matching line at 25.6 MHz, placed symmetrically about the proton Larmor frequency 14.6 MHz.

An interesting comparison can be made between the powder ENDOR simulation, Fig. 4(a), and single crystal simulation Figs. 4 (b-d). The single crystal simulations are obtained along the principal directions of the hyperfine tensor. The hyperfine and quadrupolar tensors have nearly parallel principal axes. All simulations were made at the same field position. Note that the g-anisotropy is very small in this system. The strongest intensity found at 6.3 MHz is near the high frequency transition of the three principal directions. The three lowest peak positions are near the low frequency transitions of the three directions respectively.

The experimental intensities are also reproduced quite well. As described in the theoretical section the transition moment formula (12) used in the powder summation over angles θ and φ represents the averaged moment of all molecules in the powder with the same set of θ and φ values. The significance of taking this average is demonstrated in Fig. 5. The transition moments for the ^{14}N-transitions I-IV are calculated for a single crystal direction **B** // X, as function of the $\mathbf{B}_2$-orientation in the YZ-plane, described by the angle ψ. The transitions are located at 2.42, 4.04, 4.51 and 6.11 MHz respectively. The orientational variations of the transition moments are significant enough to require that an average is taken in a powder. The relative differences, $(W^2_{max}-W^2_{min})/\ W^2_{min}*100\%$, amounts to 29, 150, 16 and 73% respectively. Here W^2_{min} and W^2_{max} refers to the minimum and maximum values of W^2 of each transition over the ψ-range. In a powder the set of radicals with the same θ and φ values will be randomly ordered with respect to the RF-field and the proper averaged moments are given by formula (12). For B // X the averaged values $\overline{W}^2$ become 4.96, 5.42, 13.92 and 14.37 respectively.

4.3 ENDOR of α-protons in the biphenyl radical cation

The simulation program has further been applied to proton ENDOR spectra of organic radicals in powders. The biphenyl radical cation, $Ph_2^{+\cdot}$, stabilized on zeolite surfaces and in frozen $CFCl_3$ has been investigated recently with ENDOR and EPR by us [3]. The matrices are polycrystalline and single crystals of sufficient size are not available. ENDOR is beneficial since the EPR spectrum in both matrices has low resolution [3]. Experimental and simulated ENDOR spectra of $Ph_2^{+\cdot}$ in $CFCl_3$ are shown in Figs. 6(a) and 6(b-d) respectively. The spectra were obtained at the centre of the EPR spectrum. The simulations were made using the parameters in table 3. The assigned lines are caused by intensity build-up at positions corresponding to principal values of the anisotropic *para* and *ortho* proton hyperfine tensors. The lines are placed symmetrically around the proton Larmor frequency, near $\nu_H \pm A_i/2$ MHz, where ν_H = 14.54 MHz. The individual spectral contributions from the *para* and *ortho* proton groups are shown in Figs. 6(c) and 6(d). Fluorine matrix nuclei and the small hyperfine couplings of *meta* protons were excluded in the simulation. They produce lines in the region 10.5 to 16.5 MHz in the experimental spectrum [3].

As can be seen from Fig. 6(a) the lines below ν_H are of lower intensity than matching lines above. We attribute this to the so called hyperfine enhancement effect, which has been discussed for ENDOR in solids by several authors [19,20,24]. In the simulations intensities are calculated to first order using Eq. (12). The relative intensity distribution is predicted but slightly overestimated in the calculated spectrum. A perfect fit might not be feasible since relaxation and instrumental effects are neglected.

Powder ENDOR from ring protons of the α-proton type have been detected in p-benzoquinone$^{\cdot-}$ in isopropyl alcohol [8], the tyrosyl radical in ribonucleotide reductase [10] and radical cations of biphenyl [3] and naphthalene[5] in frozen $CFCl_3$ and of perylene on silica- alumina [1]. In these cases the hyperfine anisotropy is of the same order as the isotropic contribution. Well resolved signals are observed despite the pronounced anisotropy since the principal components are fairly small, 5 - 30 MHz. The transitions are hence spread over a relatively small region compared to radicals with localized spin density where α-couplings are of the order 30 - 90 MHz.

5. Conclusions

The present work show that it is possible to calculate powder ENDOR spectra of radicals with perturbation theory including effects of quadrupolar interactions. For the systems tested experimental intensities are frequency dependent as predicted with first order transition moments. The use of zero order theory would here yield frequency independent intensities. The fit of calculated intensities with experiment is only approximate, primarily because relaxation effects are excluded, but in many cases it is sufficient for a spectral assignment. It should be emphasized that if transition moments are to be used to predict intensities the effect of the RF-field direction must be taken into account.

Acknowledgement

This work has been financed by the Swedish Natural Science Council (NFR).

Appendix

A. Derivation of the ENDOR transition moment

The derivation of the formula (9) from the general equation (11) is demonstrated for a single nucleus and $M_S = +½$ to simplify the notation. The derivation for a case with several nuclei is analogous. The transition moment between two states $\Phi(+½, a)$ and $\Phi(+½, b)$ is given by:

$$W = \langle\Phi(+½, a)| B_2(\beta \mathbf{rgS} - g_N\beta_N \mathbf{I}\cdot\mathbf{r}) |\Phi(+½, b)\rangle. \quad \text{(A1)}$$

The wave functions are to first order (cf. Eq. (7)):

$$\langle\Phi(+½, a)| = \langle+½, a| + \sum_c \frac{\langle +½, a|\mathcal{H}''|-½, c\rangle}{+g\beta B} \langle -½, c| \quad \text{(A2a)}$$

$$|\Phi(+½, b)\rangle = |+½, b\rangle + \sum_d \frac{\langle -½, d|\mathcal{H}''|+½, b\rangle}{+g\beta B} |-½, d\rangle \quad \text{(A2b)}$$

The nuclear states a and b are eigenstates in the $M_S = +½$ manifold (states $|v\rangle$ in Eq. (6a)). The summation indices c and d run over the $2I+1$ nuclear eigenstates in the $M_S = -½$ manifold (states $|w\rangle$ in Eq. (6b)). The electronic part of the matrix elements in the numerators can be calculated by using the shift operators $S_+$and S_- in $\mathcal{H}''$ which gives:

$$\langle +½, a|\mathcal{H}''|-½, c\rangle = \langle a|Q_+|c\rangle, \quad \text{(A3)}$$

$$\langle -½, d|\mathcal{H}''|+½, b\rangle = \langle d|Q_-|b\rangle, \quad \text{(A4)}$$

where

$$\mathcal{H}'' = \mathbf{IAp}S_p + \mathbf{IAq}S_q = Q_+S_+ + Q_-S_-. \quad \text{(A5)}$$

$$Q_\pm = \tfrac{1}{2}(\mathbf{IAp} \mp i\mathbf{IAq}). \quad \text{(A6)}$$

$$S_\pm = S_p \pm iS_q \quad \text{(A7)}$$

Using the orthogonal vectors **p**, **q**, and **u** and the S_+, S_-, and S_u operators the **rgS** operator can be written:

$$\mathbf{rgS} = \mathbf{rgp}S_p + \mathbf{rgq}S_q + \mathbf{rgu}S_u = k_+S_+ + k_-S_- + k_uS_u, \quad \text{(A8)}$$

where

$$k_\pm = \tfrac{1}{2}(\mathbf{rgp} \mp i\mathbf{rgq}), \; k_u = \mathbf{rgu}. \quad \text{(A9)}$$

Inserting (A2)-(A4), and (A8) into (A1) gives:

$$W = \frac{B_2}{B}\{ \langle +½, a| + \sum_c \frac{\langle a|Q_+|c\rangle}{+\nu_e} \langle -½, c| (\nu_e \tfrac{1}{g} (k_+S_+ + k_-S_- + k_uS_u) - \nu_N \mathbf{I}\cdot\mathbf{r}) |+½, b\rangle +$$

$$\sum_d \frac{\langle d|Q_-|b\rangle}{+\nu_e} |-½, d\rangle \}, \qquad \text{(A10)}$$

where $\nu_e = g\beta B$ and $\nu_N = g_N\beta_N B$. Keeping only the nonzero matrix elements in Eq. (A10) gives:

$$W = \frac{B_2}{B}\{ -\frac{k_u}{2g\nu_e} \sum_{cd} \langle a|Q_+|c\rangle\langle d|Q_-|b\rangle\delta_{cd} - \langle a| \nu_N \mathbf{I}\cdot\mathbf{r} | b\rangle$$

$$+\frac{1}{g}\sum_c \langle +½, a|k_+S_+ + k_-S_-|-½, c\rangle\langle c|Q_-|b\rangle$$

$$+\frac{1}{g}\sum_d \langle a|Q_+|d\rangle\langle -½, d|k_+S_+ + k_-S_-|+½, b\rangle \}. \qquad \text{(A11)}$$

In (A11) a term of order less than $\frac{B_2}{B}\nu_N(\mathrm{hfi}/\nu_e)^2$ has been neglected. Further, for modest g-anisotropy and ℓ perpendicular to $\mathbf{r}$ the first term in (A11) will be negligible. In this case:

$$k_u = \mathbf{rgu} = \frac{1}{g}\mathbf{rg}^2\boldsymbol{\ell} \approx \mathbf{gr}\cdot\boldsymbol{\ell} = 0. \qquad \text{(A12)}$$

In combination with the factor $\frac{1}{\nu_e}$ this ensures that the first term is much smaller than the other terms and can be neglected. Calculating the electronic part of the remaining matrix elements and using the closure relation in the summations over c and d we get:

$$W = \frac{B_2}{B}\{ -\langle a| \nu_N \mathbf{I}\cdot\mathbf{r} | b\rangle + \frac{1}{g}\sum_c k_+\langle a|c\rangle\langle c|Q_-|b\rangle + \frac{1}{g}\sum_d k_-\langle a|Q_+|d\rangle\langle d|b\rangle \}$$

$$= \frac{B_2}{B}\{ -\langle a| \nu_N \mathbf{I}\cdot\mathbf{r} | b\rangle + \frac{1}{g}k_+\langle a|Q_-|b\rangle + \frac{1}{g}k_-\langle a|Q_+|b\rangle \}. \qquad \text{(A13)}$$

Using the definitions (A6) and (A9) of $Q_\pm$ and $k_\pm$ and the identity:

$$\mathbf{IAgr} = (\mathbf{IAp})(\mathbf{rgp}) + (\mathbf{IAq})(\mathbf{rgq}) + (\mathbf{IAu})(\mathbf{rgu}), \qquad \text{(A14)}$$

this can be combined into a single matrix element:

$$W = \frac{B_2}{B} < a | + \frac{1}{2}\frac{1}{g}(\mathbf{I}A\mathbf{g}\mathbf{r} - (\mathbf{I}A\mathbf{u})(\mathbf{r}\mathbf{g}\mathbf{u})) - \nu_N \mathbf{I}\cdot\mathbf{r} \mid b >$$

$$\approx \frac{B_2}{B} < a | + \frac{1}{2}\frac{1}{g}\mathbf{I}A\mathbf{g}\mathbf{r} - \nu_N \mathbf{I}\cdot\mathbf{r} \mid b > \qquad \text{(A15)}$$

where we in the last step assumed that the relation (A12) is valid. The derivation for the case of $M_s = -1/2$ is analogous and yields:

$$W \approx \frac{B_2}{B} < a | - \frac{1}{2}\frac{1}{g}\mathbf{I}A\mathbf{g}\mathbf{r} - \nu_N \mathbf{I}\cdot\mathbf{r} \mid b > \qquad \text{(A16)}$$

The squared transition moment is thus given to first order by:

$$W^2 = (\frac{B_2}{B})^2 \mid < a \mid \mathbf{I}\cdot(M_s A\mathbf{g}/g - \nu_N 1)\cdot\mathbf{r} \mid b > \mid^2 \qquad \text{(A17)}$$

B. Integration of the ENDOR transition moment in a powder sample

Integration of the squared transition moment W^2, given in Eq. (9), over ψ yields:

$$\int_{\psi} W^2(\theta, \varphi, \psi) d\psi = \int_{\psi} (\frac{B_2}{B})^2 \mid < a \mid \mathbf{I}\cdot\mathbf{C}\cdot\mathbf{r} \mid b > \mid^2 d\psi =$$

$$(\frac{B_2}{B})^2 \sum_{k,l,m,n} < a \mid I_k \mid b >< b \mid I_l \mid a > \mathbf{C}_{km}\mathbf{C}_{ln}\{r_m r_n\} \qquad ; k, l, m, n = X, Y, Z \qquad \text{(A18)}$$

where

$$\{r_m r_n\} = \int_{\psi} r_m r_n d\psi \qquad \text{(A19)}$$

The nuclear index i in the state labels has been dropped for simplicity. The direction cosines, r_m and r_n, of the RF-field with respect to the molecular reference system (cf. Fig. 1) are given by:

$$r_X = \cos\theta\cos\varphi\cos\psi - \sin\varphi\sin\psi$$

$$r_Y = \cos\theta\sin\varphi\cos\psi + \cos\varphi\sin\psi \qquad \text{(A20)}$$

$$r_Z = -\sin\theta\cos\psi$$

Integration of their squares and cross products over ψ gives:

$$\{r_X^2\} = 1/2(1 - \sin^2\theta\cos^2\varphi)$$

$$\{r_Y^2\} = 1/2(1 - \sin^2\theta\sin^2\varphi)$$

$$\{r_Z^2\} = 1/2\sin^2\theta$$

$$\{r_X r_Y\} = -1/2\sin^2\theta\cos\varphi\sin\varphi \qquad \text{(A21)}$$

$$\{r_X r_Z\} = -1/2\sin\theta\cos\theta\cos\varphi$$

$$\{r_Y r_Z\} = -1/2\sin\theta\cos\theta\sin\varphi$$

The expressions (A20-21) are valid when the RF-field is perpendicular to the static magnetic field. The expressions are special cases of the more general expressions published by Kottis and Lefebvre [26]. These were derived for the mathematically related problem of the orientation of the microwave field relative to the molecule of a triplet system. The angular expressions on the right hand side in (A21) are related to the direction cosines, ℓ_X, ℓ_Y, and ℓ_Z of the static magnetic field and (A21) can be formulated as:

$$\{r_m r_n\} = 1/2(\delta_{mn} - \ell_m\ell_n) \qquad ; m,n = X, Y, Z \qquad \text{(A22)}$$

Insertion of expression (A22) into (A18) eventually gives the Eq. (12).

[1] R. B. Clarkson, R. L. Belford, K. S. Rothenberger, and H. C. Crookham, J. Catal., 106 (1987) 500 ; K. S. Rothenberger, H. C. Crookham, R. L. Belford, and R. B. Clarkson, J. Catal., 115 (1989) 430 ; R. B. Clarkson, K. Mattson, W. Shi, W. Wang and R. L. Belford, in: Radicals on Surfaces, ed. A. Lund and C. Rhodes, (Kluwer, Dordrecht, 1995), pp. 89-117

[2] Y. Wu, L. Piekara-Sady, and L. D. Kispert, Chem. Phys. Lett., 180 (1991) 573 ; L. Piekara-Sady, M. M. Khaled, E. Bradford, L. D. Kispert, and M. Plato, Chem. Phys. Lett., 186 (1991) 143 ; A. S. Jeevarajan, L. D. Kispert, and L. Peikara-Sady, Chem. Phys. Lett., 209 (1993) 269

[3] R. Erickson, A. Lund, M. Lindgren, Chem. Phys., 192 (1995) 89

[4] R. Erickson, M. Lindgren, A. Lund, and L. Sjöqvist, Colloids Surf. A, 72 (1993) 207

[5] F. Gerson and X.-Z Qin, Chem. Phys. Lett., 153 (1988) 546

[6] F. Gerson, Acc. Chem. Res., 27 (1994) 63

[7] M. Lindgren, R. Erickson, N. P. Benetis, and O. N. Antzutkin, J. Chem. Soc. Perkin Trans. II (1993) 2009

[8] P. J. O'Malley and G. T. Babcock, J. Am. Chem. Soc., 108 (1986) 3995

[9] L. R. Dalton and A. L. Kwiram, J. Chem. Phys., 57 (1972) 1132

[10] C. J. Bender, M. Sahlin, G. T. Babcock, B. A. Barry, T. K. Chandrasekar, S. P. Salowe, J. Stubbe, B. Lindström, L. Pettersson, A. Ehrenberg and B.-M. Sjöberg, 111 (1989) 8076

[11] R. LoBrutto, Y.-H. Wei, R. Mascarenhas, C. P. Scholes and T. E. King, 258 (1983) 7437

[12] G. H. Rist and J. S. Hyde, J. Chem. Phys, 52 (1970) 4633

[13] B. M. Hoffman, J. Martinsen, and R. A. Venters, J. Magn. Reson., 59 (1984) 110 ; B. M. Hoffman, R. A. Venters, and J. Martinsen, J. Magn. Reson., 62 (1985) 537 ; B. M. Hoffman and R. J. Gurbiel, J. Magn. Reson., 82 (1989) 309

[14] B. M. Hoffman, R. J. Gurbiel, M. M. Werst, and M. Sivaraja, in: Advanced EPR: Applications in Biology and Biochemistry, ed.A. J. Hoff (Elsevier, Amsterdam, 1989), pp. 541-591 ; R. J. Gurbiel, C. J. Batie, M. Sivaraja, A. E. True, J. A. Fee, B. M. Hoffman, and D. P. Ballou, Biochemistry, 28 (1989) 4861

[15] G. C. Hurst, T. A. Henderson, and R. W. Kreilick, J. Am. Chem. Soc., 107 (1985) 7294 ; T. A. Henderson, G. C. Hurst, and R. W. Kreilick, J. Am. Chem. Soc., 107 (1985) 7299

[16] G. P. Gochev and N. D. Yordanov, J. Magn. Reson., 102 (1993) 180

[17] A. Kreiter and J. Hüttermann, J. Magn. Reson., 93 (1991) 12

[18] C. P. Keijzers, E. J. Reijerse, P. Stam, M. F. Dumont, and M. C. M. Gribnau, J. Chem. Soc. Faraday. Trans. 1, 83 (1987) 3493

[19] K. Toriyama, K. Nunome, and M. Iwasaki, J. Chem. Phys., 64 (1976) 348

[20] A. Schweiger and Hs. H. Günthard, Chem. Phys., 70 (1982) 1

[21] M. Iwasaki, J. Magn. Reson., 16 (1974) 417 ; J. A. Weil, J. Magn. Reson., 18 (1975) 113 ; A. Schweiger, F. Graf, G. Rist, and Hs. H. Günthard, Chem. Phys., 17 (1976) 155

[22] K.-Å. Thuomas and A. Lund, J. Magn. Res., 22 (1976) 315 ; A. Lund, K.-Å. Thuomas and J. Maruani, J. Magn. Res., 30 (1978) 505

[23] R. Erickson and A. Lund, J. Magn. Reson., 92 (1991) 146

[24] D. H. Whiffen, Mol. Phys. 10 (1966) 595

[25] N. M. Atherton, Principles of Electron Spin Resonance (Ellis Horwood, Chichester, 1993) pp. 214-217

[26] P. Kottis and R. Lefebvre, J. Chem. Phys., 39 (1963) 393

[27] R. Lefebvre and J. Maruani, J. Chem. Phys., 42 (1965) 1480

[28] K. Möbius and W. Lubitz, in: Biological Magnetic Resonance, Vol. 7, ed. L.J. Berliner and J. Reuben, (Plenum, New York, 1987) pp. 129-247

[29] V. P. Chacko, C. A. McDowell, and B. C. Singh, J. Chem. Phys., 72 (1980) 4111

TABLE 1
Spin Hamiltonian parameters[a] used in the powder ENDOR simulation of ^{14}NO-ligated ferrocytochrome *c* heme a_3.

Tensor	Principal value[b]	Direction cosines		
		X	Y	Z
g	2.082	1	0	0
	1.979	0	1	0
	2.008	0	0	1
A(^{14}N-His)	16.5	1	0	0
	16.1	0	1	0
	19.3	0	0	1
Q(^{14}N-His)	+0.67	1	0	0
	-1.12	0	1	0
	+0.45	0	0	1
A(^{14}NO)	30.56	1	0	0
	30.56	0	0.9537	0.3007
	59.90	0	-0.3007	0.9537
Q(^{14}NO)	+1.03	1	0	0
	-0.51	0	1	0
	-0.52	0	0	1

[a] From Refs. 11 and 17.
[b] Hyperfine and quadrupolar values in MHz.

TABLE 2
Comparison of experimental and calculated[a] values of ENDOR powder peak positions observed at the field position g = 2.086 of NO-ligated ferrocytochrome *c* oxidase heme a_3.

Nitrogen nuclei	Observed position[b] (MHz)	Calculated position[c] (MHz)	Calculated position[d] (MHz)
^{14}N(His)	6.57	6.69	6.68
	8.02	7.99	7.92
	8.51	8.65	8.60
	9.92	9.91	9.86
^{14}NO	12.76	12.91	12.94
	14.69	14.70	14.70
	15.70	15.82	15.76
	17.96	17.86	17.92

[a] Spin Hamiltonian parameters are given in table 1. Simulation parameters are as in Ref. 17; the field setting was 3.1913 mT and the microwave frequency 9.32 GHz. The weight function *s* (Gaussian shaped) had a line width of 0.5 mT. A line width of 0.35 MHz was used for the convolution function *t*, (Lorentzian shaped).
[b] Ref. 11.
[c] This work.
[d] Ref. 17.

TABLE 3

Spin Hamiltonian Parameters of $\dot{C}H_2NHCOC_6H_5$ in Hippuric Acid and of [Biphenyl]$^{\bullet+}$ in $CFCl_3$.

Paramagnetic system	Tensor	Principal value[a]	Direction cosines[b]		
			X	Y	Z
$\dot{C}H_2NHCO$-C_6H_5 in Hippuric Acid[c]	g(isotropic)	2.0028			
	$A(H_{\alpha 1})$	-24.22	∓0.496	±0.792	0.357
		-48.70	±0.072	∓0.372	±0.926
		-81.20	±0.866	±0.484	0.128
	$A(H_{\alpha 2})$	-25.46	∓0.413	∓0.847	-0.334
		-48.98	±0.081	∓0.400	0.913
		-79.06	∓0.908	±0.350	0.234
	$A(^{14}N)$	-7.58	±0.185	∓0.432	0.883
		-8.47	0.983	±0.057	∓0.178
		-9.44	±0.027	0.900	±0.435
	$Q(^{14}N)$	-0.843	±0.195	∓0.398	0.896
		+0.582	0.980	±0.128	∓0.157
		+0.261	∓0.050	0.909	±0.415
[Biphenyl]$^{\bullet+}$ in $CFCl_3$[d]	g	2.0030	1	0	0
		2.0021	0	1	0
		2.0022	0	0	1
	A(para) x 2H	-26.9	1	0	0
		-7.9	0	1	0
		-18.3	0	0	1
	A(ortho) x 4H	-12.2	±0.3771	0.9262	0
		-4.4	0.9262	∓0.3771	0
		-10.0	0	0	1

[a] Hyperfine and quadrupolar values in MHz.

[b] In hippuric acid four different sign combinations refer to four inequivalent sites in the crystal. In biphenyl two sign cominations refer to the two inequivalent groups of two ortho protons each.

[c] Parameters adapted from Ref. 29 The weak hyperfine couplings of the ring protons were excluded in the ENDOR simulation but can be found in Ref. 29.

[d] From Ref. 3

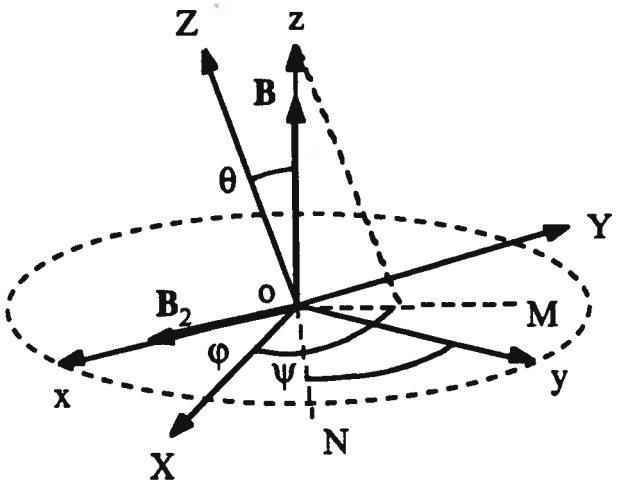

Figure 1. The relation between the molecular reference system *oXYZ* and the fixed reference system *oxyz*. The symbol **B** is the static magnetic field and $\mathbf{B}_2$ is the RF-field, linearly polarised perpendicular to the static field. Angles θ and φ are the polar co-ordinates of **B** in the molecular system. The *oN*-line is the intersection between the *xy* and *XY*-planes. Angle ψ relates the orientation of the molecular system relative to $\mathbf{B}_2$ for a given set of θ and φ. The *oM*-line is the projection of the *z*-axis in the *XY*-plane.

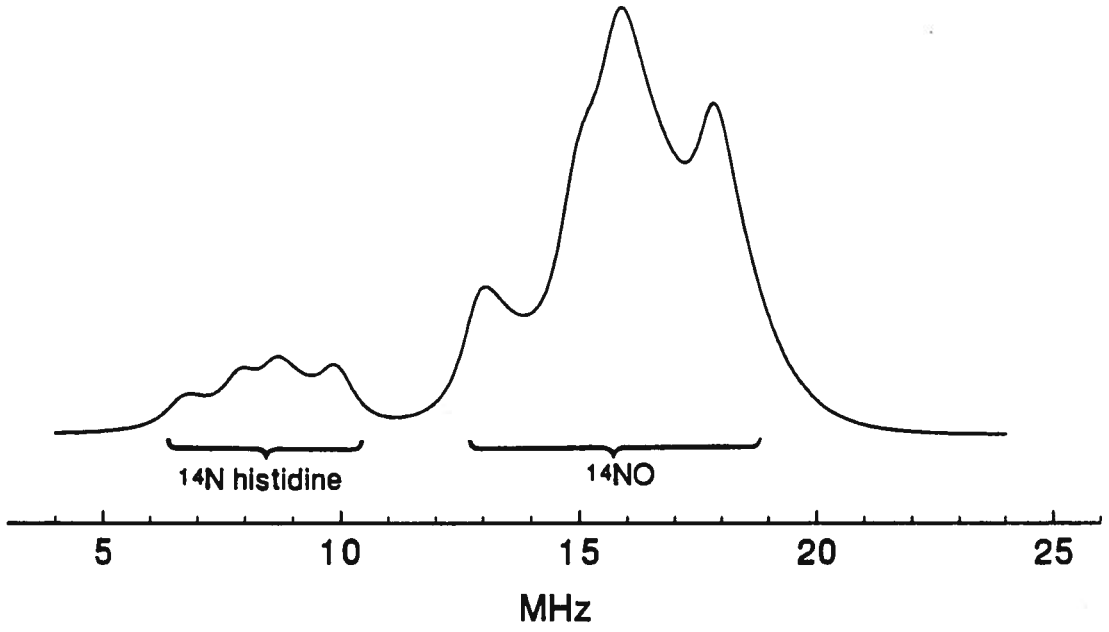

Figure 2. Simulated powder ENDOR spectrum of ^{14}NO-ligated ferrocytochrome *c* heme a_3, at the field setting g = 2.079 with $\nu_{microwave}$ = 9.32 GHz. The simulation employed the parameters of table 1. The weight function *s* (Gaussian shape) had a line width of 0.6 mT and the convolution function *t* (Lorenztian shape) had a line width of 0.5 MHz.

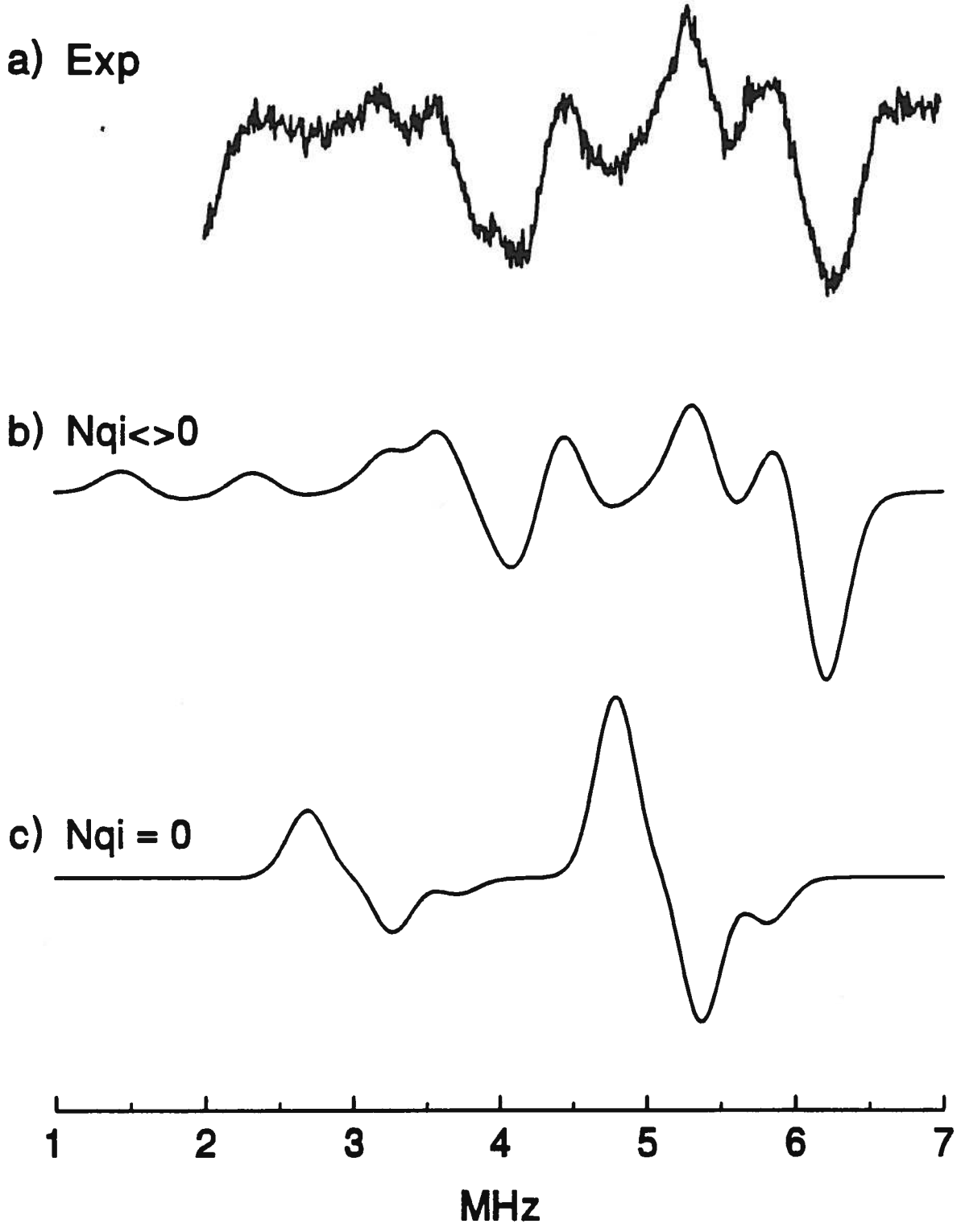

Figure 3. Experimental (a) and simulated (b), (c) powder ENDOR spectra at 110 K of X-irradiated hippuric acid. Only the region of ^{14}N-signals is shown. The spectra were obtained with $\nu_{microwave}$ = 9.57367 GHz at B = 341.53 mT at the centre of the EPR spectrum (not shown). Simulations employed the parameters of table 3. The simulations were made including (b) and excluding (c) the nuclear quadrupolar interaction, nqi. The weight function *s* (Gaussian shape) had a line width of 0.1 mT and the convolution function *t* (Lorenztian shape) had a line width of 0.5 MHz.

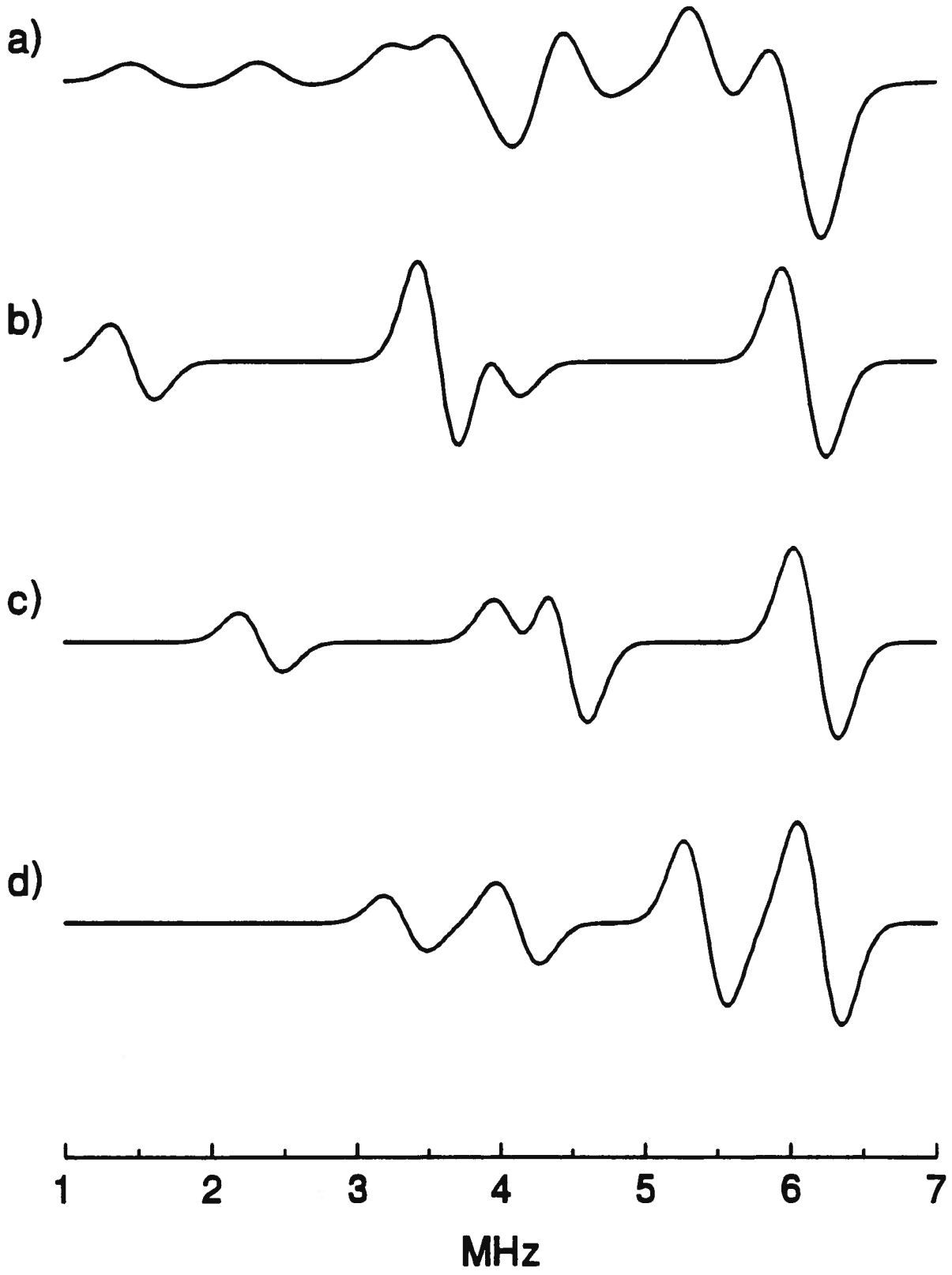

Figure 4. Comparison of simulated powder (a) and single crystal (b)-(d) ^{14}N-ENDOR spectra of the $\dot{C}H_2NHCOC_6H_5$ radical formed in hippuric acid. All spectra were obtained using the parameters of table 3 at the field and microwave frequency given in Fig. 3. Convolution parameters are as in Fig. 3. The single crystal spectra (b)-(d) were calculated with the **B**-field directed along the principal directions corresponding to the -7.58, -8.47 and -9.44 MHz nitrogen hyperfine values respectively, see table 3. The site employed corresponds to the upper sign combination in the direction cosines of table 3. Note that the principal directions of the A and Q tensors are nearly parallel.

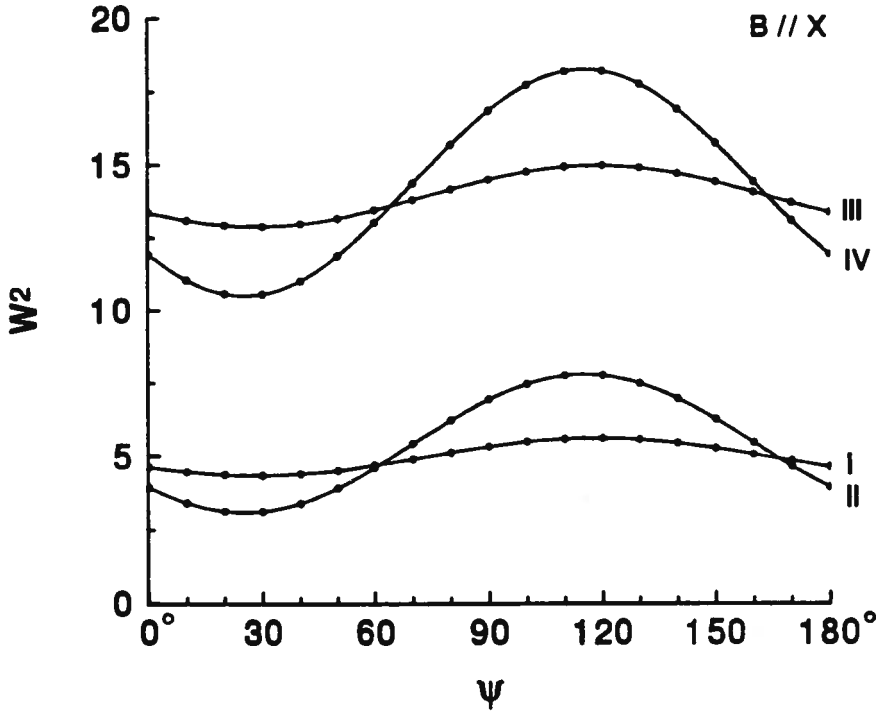

Figure 5. The square of the transition moments (arbitrary units) for the four ^{14}N-ENDOR transitions I-IV of the $\dot{C}H_2NHCOC_6H_5$ radical as function of the RF-field orientation. The calculation was made for the same site as in Fig. 4. Transition moments were calculated to first order using Eq. (9), see text. The static field was aligned along the crystallographic *X*-axis. The RF-field was linearly polarized along *x* in the *YZ*-plane, see fig 1. The angle ψ measures the direction of the RF-field in the *YZ*-plane. The transitions I-IV were located at 2.42, 4.04, 4.51 and 6.11 MHz respectively.

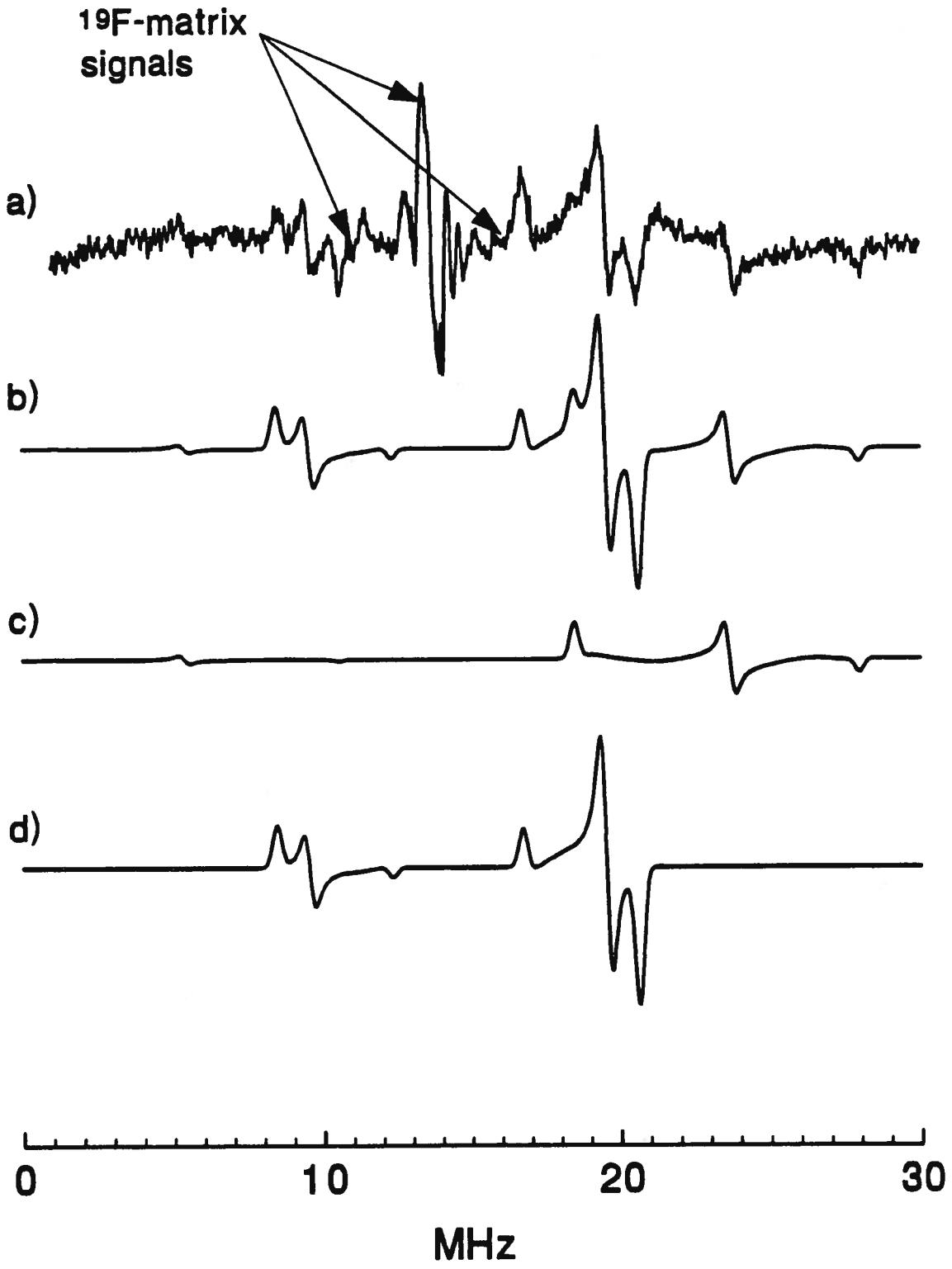

Figure 6. Experimental (a) and simulated (b)-(d) powder ENDOR spectra of the biphenyl radical cation in $CFCl_3$ matrix at 120K. The simulated spectra were calculated using the parameters of table 3 with B = 341.40mT and $\nu_{microwave}$ = 9.5670 GHz. Matrix fluorine and *meta* protons were excluded in the simulation, see text. The weight function *s* and the convolution function *t* of Eq. (13) had line widths of 0.1 mT and 0.3 MHz respectively (both Gaussian shaped). Simulation (b) show the total spectrum while (c) and (d) show the individual contributions from the *para* and *ortho* proton groups respectively.